CELL ADHESION

Competition Between Nonspecific Repulsion and Specific Bonding

GEORGE I. BELL, MICAH DEMBO, AND PIERRE BONGRAND
Theoretical Division, Los Alamos National Laboratory, University of California, Los Alamos, New Mexico 87545

ABSTRACT We develop a thermodynamic calculus for the modeling of cell adhesion. By means of this approach, we are able to compute the end results of competition between the formation of specific macromolecular bridges and nonspecific repulsion arising from electrostatic forces and osmotic (steric stabilization) forces. Using this calculus also allows us to derive in a straightforward manner the effects of cell deformability, the Young's modulus for stretching of bridges, diffusional mobility of receptors, heterogeneity of receptors, variation in receptor number, and the strength of receptor-receptor binding. The major insight that results from our analysis concerns the existence and characteristics of two phase transitions corresponding, respectively, to the onset of stable cell adhesion and to the onset of maximum cell-cell or cell-substrate contact. We are also able to make detailed predictions of the equilibrium contact area, equilibrium number of bridges, and the cell-cell or cell-substrate separation distance. We illustrate how our approach can be used to improve the analysis of experimental data, by means of two concrete examples.

INTRODUCTION

There are many well-documented systems in which the presence of specific molecules (CAMs, SAMs, lectins, antibodies, etc.) are required for cell-cell or cell-surface adhesion to occur (Frazier et al., 1982; Edelman, 1983; Springer and Barondes, 1982). Furthermore, even in instances where a chemical species responsible for formation of cell-cell bridges is unknown (e.g., T-killer-target binding), the specificity of the interactions indicates that specific receptors are necessary for cell adhesion. The fact that cells do not stick to each other or to surfaces unless a substantial number of specific cell-cell bridges can form, argues for the existence of a repulsive barrier that must somehow be overcome by bridging molecules. The existence of a repulsive barrier preventing adhesion is further emphasized by studies showing that even when numerous bridging molecules are present, cells must frequently be forced into close contact by centrifugation before strong bonding occurs (Capo et al., 1982). Moreover, it was shown by Grinnell (1974) that centrifugation could bypass several metabolic steps otherwise required for bonding.

Given the existence of a repulsive barrier, Fig. 1 illustrates a very minimal account of the various kinds of energetic states that can occur during the interaction of two cells. If the cells are far apart (Fig. 1 *a*), then the free energy of the system will be a simple sum of independent contributions from the individual cells. In contrast, if the cells move closer to each other, the attractive and repulsive interactions will cause the free energy of the system to depend on interactions between the cells. Certain configurations will be unfavorable because of the repulsive barrier (Fig. 1 *b*). In other configurations the repulsive interaction will be counterbalanced by the formation of cell-cell bridges (Fig. 1 *c*). As illustrated in Fig. 1 *c*, a configuration involving redistribution of receptors into the contact region might be required to achieve a degree of bridging sufficient to overcome the repulsive barrier.

The complex balance between specific bonding and nonspecific repulsion that governs the mutual interactions of two adhering cells is difficult to understand on a simple intuitive level. The complexity of adhesion argues the need for a general modeling language applicable to the analysis of the wide spectrum of natural and experimental systems in which cell adhesion plays a role. The present work was motivated by the realization that, despite the manifestly nonequilibrium nature of real cells, when properly formulated and applied, a variety of thermodynamic concepts can provide a basis for such a modeling language.

An equilibrium thermodynamic language for describing cell-cell interactions must tacitly assume that the chemical and physical processes included in the description, equilibrate on time scales that are short compared with the scales required for metabolic changes that tend to drive the system away from equilibrium. In particular, Fig. 1 implies that the times required for passive processes (e.g., diffusion of receptors into the contact region, variation of the cell-cell separation distance, and formation of cell-cell bridges [Bell, 1978, 1979]) are in some sense fast com-

P. Bongrand's address is Laboratoire d'Immunologie, Hôpital Sainte Marguerite, B. P. 29, 13277 Marseilles Cedex 09, France.

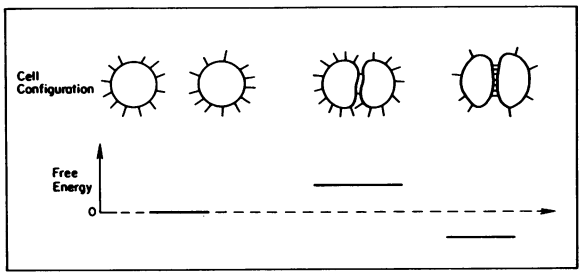

FIGURE 1 When two cells first come into contact, the free energy is increased (*center*) and only after receptors have accumulated in the contact area (*right*) is the free energy below that of the separated cells.

pared with the time scales of metabolically powered processes (e.g., synthesis of new receptors, modulation of cytoskeletal architecture, changes in the repulsive barrier). We cannot claim to have proven that this fundamental requirement for a thermodynamic model is met in every instance of cell adhesion; nevertheless, it is a sufficiently mild requirement that we will proceed with the analysis and judge its validity by empirical comparison with experiment.

To illustrate the thermodynamic approach to the modeling of adhesion, we first present the detailed formulation and analysis of a representative example called adhesion model No. 1 (AM-1). We will then indicate how the various elements of AM-1 can be varied and generalized to create a very large class of related models each applicable to different circumstances. Finally, we attempt to demonstrate the analytical and predictive utility of our approach by comparing the predictions of AM-1 and related models with data on adhesion of cells under various experimental circumstances.

ADHESION MODEL NO. 1

Free Energy Function

Consider two cells with mutually complementary receptors and assume that the receptors on each cell are freely mobile in the entire plane of the membrane and that the receptors constitute a minor fraction of the total membrane mass. This implies that receptors will behave as ideal solute particles in the lipid bilayer and that unless cell-cell contact induces redistribution into the contact region, the receptors will be uniformly distributed over the entire cell surface.

Fig. 2 illustrates our idealized view of the geometry of cell-cell contact. Within a certain well-defined set of contact points $\{A\}$, the cells are separated by a small distance S. Outside the contact region the cells are separated by a distance much greater than S. According to Fig. 2, if $\mathbf{x}$ denotes an arbitrary location on the surfaces of cell 1 or cell 2, then either $\mathbf{x}$ represents a point belonging to the set of contact points ($\mathbf{x} \in \{A\}$) or $\mathbf{x}$ represents a location outside of the contact region, on the free surfaces of cells 1 or 2, ($\mathbf{x} \in [\{A_1\} - \{A\}]$ or $\mathbf{x} \in [\{A_2\} - \{A\}]$).

Fig. 2 is quite purposely ambiguous about the shape and topology of the set of contact points and about what happens at the boundary of the contact region. In AM-1 we have neglected a thin transition zone where the cell-cell separation distance is larger than S and yet is not quite so large as to be effectively infinite. AM-1 also neglects the possibility that there might be two or more distinct contact distances (e.g., close contacts and very-close or focal contacts).

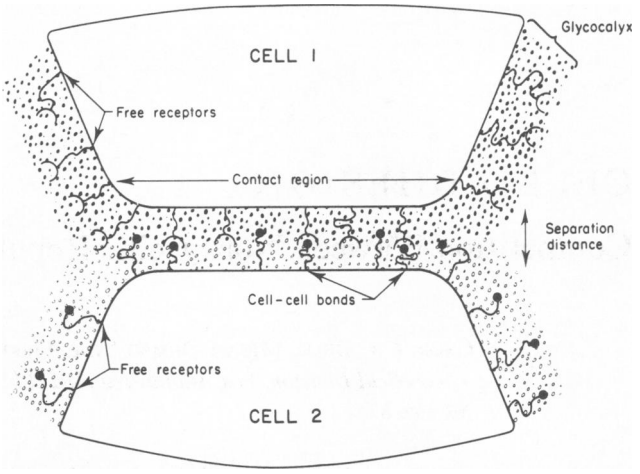

FIGURE 2 Model for the interaction of cell surface molecules in the region of cell contact. In the contact area, nonspecific repulsion is mediated by interaction between the hydrophilic polymers associated with the cell surface. The repulsive forces are counterbalanced by formation of bridges between mobile surface receptors.

For adhesion to occur, the separation distance within the contact region must be sufficiently small to allow bonding between the complementary receptors on the two cells; by definition such bonds cannot form outside the contact region. We will denote the local surface density of receptors at a position $\mathbf{x}$, by $n_{1t}(\mathbf{x})$ for receptors on cell No. 1 or $n_{2t}(\mathbf{x})$ for receptors on cell No. 2. Because receptors can only be in one of two states, free or bonded, we surmise that for any location

$$n_{1t}(\mathbf{x}) = n_1(\mathbf{x}) + n_b(\mathbf{x}) \tag{1a}$$

and

$$n_{2t}(\mathbf{x}) = n_2(\mathbf{x}) + n_b(\mathbf{x}), \tag{1b}$$

where the $n_i(\mathbf{x})$, $i = 1, 2$, are the local surface densities of unattached receptors and $n_b(\mathbf{x})$ is the local surface density of cell-cell bridges.

According to AM-1, bridges cannot occur outside the set $\{A\}$; whereas inside $\{A\}$ all points are energetically equivalent. This implies that to maximize entropy, the surface density of cell-cell bridges must be a positive constant inside the contact region and zero outside the contact region. Obviously, if A is the area of the set $\{A\}$ and N_b represents the absolute number of bridges holding the two cells together, then the uniform density of bridges in the contact region is

$$n_b(\mathbf{x}) = n_b = N_b/A \qquad \mathbf{x} \in \{A\}. \tag{1c}$$

In contrast to bound receptors, the free receptors on cell 1 or cell 2 can exist with equal probability at any point on the cell surface, both inside and outside the contact region. Thus sufficiently near thermal equilibrium, free receptors on cells 1 and 2 will be uniformly distributed over the entire cell surface. Using this fact, it is easy to show that if N_{1t}, A_1, N_{2t}, and A_2 represent the total numbers of receptors and the total surface areas of cells 1 and 2, then

$$n_1(\mathbf{x}) = n_1 = (N_{1t} - N_b)/A_1 \qquad \mathbf{x} \in \{A_1\} \tag{2a}$$

and

$$n_2(\mathbf{x}) = n_2 = (N_{2t} - N_b)/A_2 \qquad \mathbf{x} \in \{A_2\}. \tag{2b}$$

We are now in a position to consider the change in Gibbs free energy of the closed system containing two cells during a process in which the cells go from a separated state, where they do not interact, to a bound state,

where nonspecific repulsion and formation of cell-cell bridges occur. For such a process[1]

$$\Delta G = [(N_{1t} - N_b)\mu_1(n_1) - N_{1t}\mu_1(N_{1t}/A_1)] + [(N_{2t} - N_b)\mu_2(n_2) - N_{2t}\mu_2(N_{2t}/A_1)] + N_b\mu_b(n_b, S) + A\Gamma(S). \quad (3)$$

In order of their appearance the various terms in Eq. 3 represent (*a*) the free-energy change undergone by unattached receptors on cell No. 1 due to bond formation ($\mu_1[n_1]$ denotes the chemical potential of a free receptor on cell No. 1), (*b*) the free-energy change for free receptors on cell No. 2 ($\mu_2[n_2]$ is the chemical potential of a free receptor on cell No. 2); (*c*) the free energy of the cell-cell bridges ($\mu_b[n_b,S]$ is the chemical potential of a cell-cell bridge), and (*d*) the work done in overcoming the nonspecific repulsion between the cells ($\Gamma[S]$ in the free energy of nonspecific repulsion per unit area of contact). Notice, that in light of Eqs. 1, 2a, and 2b, the various terms in Eq. 3 can all be expressed as functions of only three independent variables N_b, A, and S.

By definition, a state of a closed system will be stable only if it corresponds to a choice of the independent variables for which ΔG has a relative minimum. Thus by finding the minima of Eq. 3 with respect to N_b, A, and S we can determine the number of distinct stable states of two adhering cells as well as the most probable equilibrium properties of these states. However, to proceed with an analysis of the free energy function, we must first obtain explicit expressions for the chemical potentials and for the potential energy of nonspecific repulsion.

Chemical Potentials

According to AM-1, the chemical potential for each species of free receptor can be written in the ideal solution form (e.g., Hill, 1960)

$$\mu_i(n_i) = \mu_i^0 + kT\ln(n_i) \qquad i = 1, 2. \quad (4)$$

In a similar way the chemical potential of cell-cell bridges is given by

$$\mu_b(n_b, S) = \mu_b^0(S) + kT\ln(n_b). \quad (5a)$$

In Eqs. 4 and 5a, the μ_i^0, $i = 1, 2, b$, represent the chemical potentials of free or bound receptors at some standard surface density, e.g., 1 molecule/μ^2. μ_1^0 and μ_2^0 are simply contants because the internal energy of free receptors is assumed to be unaffected by the geometry of cell contact; in contrast $\mu_b^0(S)$ is variable because the internal energy of cell-cell bridges depends quite critically on the cell-cell separation distance.

The physical basis for the S-dependence of μ_b^0 is illustrated in Fig. 3. As indicated by this figure, cell-cell bridges must have a natural, unstressed length that corresponds to a state of minimum internal energy. If the separation distance is larger or smaller than the unstressed bridge length, then bonds will be either stretched or compressed. Just as when a spring is stretched or compressed, deformation of cell-cell bridges must increase their internal energy leading to the S dependence of μ_b^0. It is clear from this analogy with a spring that if L is the natural length of a cell-cell bridge, then, by Taylor's Theorem

$$\mu_b^0(S) = \mu_b^0(L) + \tfrac{1}{2}\kappa(S - L)^2 + \ldots, \quad (5b)$$

where κ is the spring constant for stretching of the bridges. In AM-1 we neglect the higher order terms in Eq. 5b.

If we imagine that the receptors are typical glycoprotein molecules, then Fig. 3 can be interpreted as follows. In the unstressed state, Fig. 3 *a*, the receptors are viewed as somewhat globular compact structures. With stress, the binding sites may begin to deform and eventually rupture (Bell, 1978) without noticeable deformation of the receptor as a whole. In this case, the constant, κ, will be relatively large. Alternatively, under stress, the receptors may begin to unfold or denature. This process might lead to eventual disruption of the binding site, at least if the site involves determinants of the molecule that became dispersed during denaturation. In this case, κ could be relatively small, indicating the possibility of substantial receptor stretching before bond rupture.

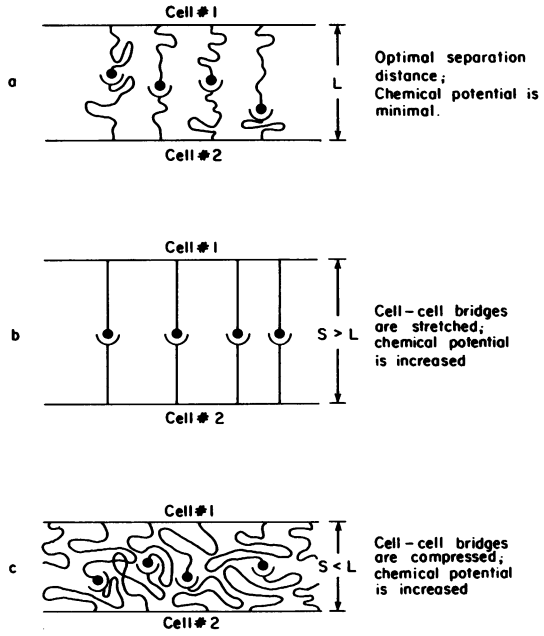

FIGURE 3 Cell-cell bridges have an optimum average length, L, for which chemical potential is minimal.

By analogy with the classical equilibrium constant for solution phase rectants, we can define an equilibrium constant for cell-cell bridging at a given separation distance

$$K(S) \equiv \exp\{[\mu_1^0 + \mu_2^0 - \mu_b^0(S) + kT]/kT\} \approx K_L \exp[-\tfrac{1}{2}\kappa(S - L)^2/kT]. \quad (6a)$$

This equilibrium constant will be shown to determine the density of cell-cell bonds in the usual way (cf., Eq. 10a).

As intuition suggests, $K(S)$ reaches its maximum value, K_L, when the separation distance is equal to the unstressed length of the bonds. Physically, K_L represents the binding constant for formation of an unstressed cell-cell bridge. Usually it is sufficient to think of K_L as a constant that depends only on the internal structure of the two receptor species. However, if a competitive inhibitor of the receptors on one of the cells is present, then it can be easily shown that the inhibition of binding can be fully taken into account by defining an effective value of K_L that depends on the concentration of inhibitor; all other parameters of adhesion remain unaffected. In exact parallel with the effect of inhibition on ordinary receptor-ligand binding, if I is the inhibitor concentration in solution and K_i is the dissociation constant of the receptor ligand complex, then the dependence of the binding constant on I is given by

$$K_L(I) = K_L(0)/(1 + I/K_i), \quad (6b)$$

where $K_L(0) \equiv K_L$ is the value of the binding constant in the absence of inhibition.

Repulsive Potential

$\Gamma(S)$ in Eq. 3 represents the mechanical work that must be done against nonspecific repulsive forces to bring a unit area of membrane from an infinite separation to a separation distance of S. If the nonspecific

[1]More properly, we could write $\Delta G = \int \mu(n)dN$, but all terms, depending on concentration, would be as in Eq. 3.

repulsive force at distance S is given by $F(S)$, then

$$F(S) = -\Gamma'(S), \tag{7a}$$

or equivalently

$$\Gamma(S) = \int_S^\infty F(s)\mathrm{d}S. \tag{7b}$$

According to recent estimates (Bongrand and Bell, 1984; Bongrand et al., 1982) the attractive electrodynamic forces between cells are negligible and the repulsive barrier between cells arises mostly from a combination of two effects (*a*) electrostatic repulsion between negative charges associated with the cell surfaces and (*b*) the so-called steric stabilization effect. The steric stabilization force is well-known in the theory of colloid suspensions (Napper, 1977); it arises because cell membranes are coated by a hydrated layer of long-chain polymer molecules (i.e., the glycocalyx). As two such polymer-coated surfaces approach each other, the polymer layers overlap and some of the water of hydration is squeezed out of the intercellular gap (see Fig. 4). The repulsive force results from a combination of the osmotic tendency of solvent to return into the intercellular space, and the steric compression of the polymer chains.

In AM-1 we adopt a simple phenomenological equation for $\Gamma(S)$ that is a smoothed representation of an expression derived for idealized membranes by Bongrand and Bell (1984)

$$\Gamma(S) = \frac{\gamma}{S}\exp\left(-\frac{S}{\tau}\right). \tag{8}$$

Qualitatively, the repulsive energy falls roughly as the reciprocal of the separation distance out to a distance τ, after which it drops more rapidly. Both the steric stabilization force and the electrostatic repulsion are expected to have roughly this shape.

From a descriptive point of view, the parameter γ in Eq. 8 is a measure of the ease with which the polymer layer between cells 1 and 2 can be compressed. Theoretical estimates of γ can be derived by considering the

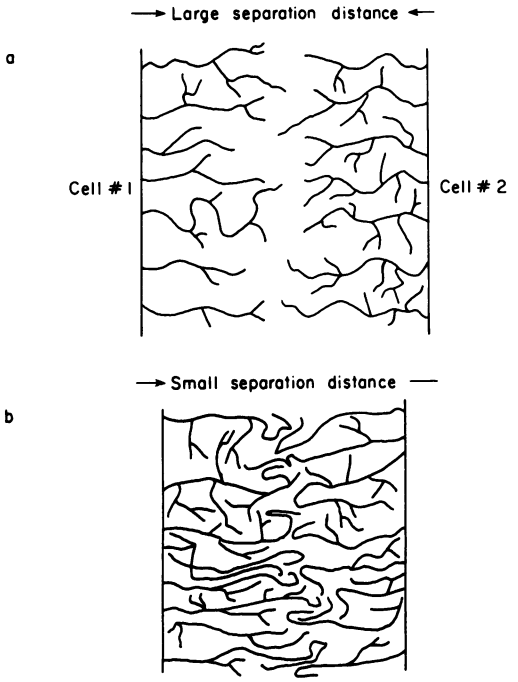

FIGURE 4 Interaction between the glycocalyces of two neighboring cells is generally repulsive due to electrostatic repulsion, solvent exclusion, and polymer compression at small separation distances between the plasma membranes.

statistical mechanics of chain molecules anchored to rigid surfaces (Napper, 1977). For typical cell parameters such estimates yield values for γ on the order of 10^{-6}–10^{-5} dyn (Bongrand and Bell, 1984). The parameter τ is a measure of the combined thickness of the polymer layers on the two cells; for typical cell-cell or cell-surface interactions τ will be between 5 and 30 nm.

Note that our views regarding the magnitude of the intercellular repulsion are at variance with the estimates of some earlier authors (Parsegian, 1973; Nir and Anderson, 1977; Gingell and Vince, 1980) who had estimated that van der Waals attraction may even overcome a weak electrostatic repulsion, for cell separations $\gtrsim$5 nm. The differences are due to neglect of steric stabilization effects by these authors and also because in estimating the electrostatic repulsion, we have assumed a uniform volume distribution of negative charge (in a 10 nm thick layer outside the plasma membrane) rather than a surface distribution. Insofar as much of the charge is associated with sialic acids on glycoproteins and other extended macromolecules, we believe the volume distribution is a more reasonable approximation.

Minimization of Free Energy

Although they are free to vary independently, N_b, A, and S must still satisfy certain a priori constraints. For example, since the separation distance must be strictly greater than zero, we require that

$$0 < S < \infty. \tag{9a}$$

In addition, since the number of cell-cell bridges cannot increase if there are no free receptors left on one of the cells, we must constrain N_b to satisfy the inequality

$$0 \leqq N_b \leqq \min\,(N_{1t}, N_{2t}). \tag{9b}$$

In a similar way, it is clear that the area of contact between two cells cannot increase if the larger of the two cells has completely surrounded the smaller. In addition to this obvious restriction, the area of contact between two cells could be subject to more demanding constraints. For example, if the cells are of nearly equal area, the contact area cannot approach the cell area since each cell must have an appreciable interface with the environment. Moreover, if the cell membranes are supported by rigid internal structures, then the two surfaces might not be able to deform or bend sufficiently to increase contact beyond a certain point. Such a situation probably occurs if contact between cells takes place by means of a specialized cell extension or pseudopod (e.g., neuron-dendrite adhesion). In light of this type of possibility, the contact area between two cells will in general be subject to a constraint of the form

$$0 \leqq A \leqq A_{\max} \leqq \min\,(A_1, A_2). \tag{9c}$$

At thermal equilibrium ΔG will be a minimum with respect to variations in all the independent variables. However, if $\bar{A}$, $\bar{N}_b$, and $\bar{S}$ represent the values of the independent variables that give the lowest permissible value of ΔG, then because of the a priori constraints, these quantities do not necessarily correspond to the values of the variables that give the absolute minimum value of ΔG ($\hat{\mathrm{A}}$, $\hat{\mathrm{N}}_b$, and $\hat{\mathrm{S}}$). Depending on whether $\hat{\mathrm{A}}$, $\hat{\mathrm{N}}_b$, and $\hat{\mathrm{S}}$ violate one or another of the constraint conditions, the system can display several different stable modes of behavior (i.e., several phases).

Because ΔG is a continuously differentiable function $\hat{\mathrm{N}}_b$, $\hat{\mathrm{A}}$, and $\hat{\mathrm{S}}$ must satisfy the three simultaneous equations $\partial_{N_b}\Delta G = \partial_A \Delta G = \partial_S \Delta G = 0$. Using Eqs. 4, 5a, and 8 to express the chemical potentials and the repulsive potential in terms of N_b, A, and S, the conditions for an absolute minimum of ΔG can be put in the form

$$\frac{N_b}{A} = \left(\frac{N_{1t} - N_b}{A_1}\right)\left(\frac{N_{2t} - N_b}{A_2}\right)K(S) \tag{10a}$$

$$\frac{N_b}{A} = \frac{\Gamma(S)}{kT} \approx \left(\frac{\gamma}{kTS}\right)\exp\,[-S/\tau] \tag{10b}$$

and

$$\frac{N_b}{A} = -\frac{\left[\frac{d}{dS}\Gamma(S)\right]}{\left[\frac{d}{dS}\mu_b^0(S)\right]} \approx \frac{\gamma(S+\tau)\exp[-S/\tau]}{\kappa\tau S^2(S-L)}. \quad (10c)$$

To solve Eqs. 10a, b, and c, we first subtract Eq. 10b from 10c. Then, noting that the resulting expression can be put in the form of a simple quadratic in S, we conclude that

$$\hat{S} = \frac{1}{2}\left[L + \frac{kT}{\kappa\tau} + \sqrt{\left(L + \frac{kT}{\kappa\tau}\right)^2 + \frac{4kT}{\kappa}}\right]. \quad (11)$$

Finally, since Eq. 11 fixes $\hat{S}$, $\hat{N}_b$, and $\hat{A}$ can be obtained by solving Eqs. 10a and 10b, regarding $\Gamma(\hat{S})$ and $K(\hat{S})$ as known parameters. When this is done we obtain

$$\hat{N}_b = \tfrac{1}{2}\left[N_{1t} + N_{2t} - \sqrt{(N_{1t} - N_{2t})^2 + 4\xi(\hat{S})}\right] \quad (12a)$$

and

$$\hat{A} = \frac{kT}{2\Gamma(\hat{S})}\left[N_{1t} + N_{2t} - \sqrt{(N_{1t} - N_{2t})^2 + 4\xi(\hat{S})}\right], \quad (12b)$$

where $\xi(S)$ is a nondimensional parameter that measures the ratio of repulsion to binding

$$\xi(S) \equiv A_1A_2\Gamma(S)/kTK(S). \quad (13)$$

Examination of Eqs. 12a and b demonstrates that if

$$\xi(\hat{S}) > N_{1t}N_{2t}, \quad (14)$$

then both $\hat{A}$ and $\hat{N}_b$ will be less than zero. Thus if Eq. 14 holds, Eqs. 12a and b obviously do not give permissible values of A and N_b.

In a similar way, it can easily be verified from Eq. 12a that if

$$\xi(\hat{S}) \leq \left[\mathrm{Min}(N_{1t}, N_{2t}) - \frac{\Gamma(\hat{S})A_{max}}{kT}\right] \left|\mathrm{Max}(N_{1t}, N_{2t}) - \frac{\Gamma(\hat{S})A_{max}}{kT}\right|, \quad (15)$$

then $\hat{A} > A_{max}$, in violation of the upper limit of Eq. 9c. On the other hand, if neither Eq. 14 nor Eq. 15 holds, then the values of $\hat{S}$, $\hat{N}_b$, and $\hat{A}$, given by Eqs. 11, 12a, and 12b, will be consistent with all the a priori constraint conditions; in this case the permissible minimum and the absolute minimum of ΔG coincide.

It is clear from Eqs. 14 and 15, that the nondimensional parameter $\xi(\hat{S})$ plays a critical role in determining the phase of the thermodynamic system formed by two adhering cells. This is illustrated geometrically by considering the typical structure of a phase diagram in the plane defined by coordinates $\xi(\hat{S})$ and N_{1t} (see Fig. 5). The inequalities, Eq. 14 and 15, lead to a division of the phase diagram into three regions. The boundary between regions I and II is formed by the straight line through the origin $\xi = N_{2t}N_{1t}$. The boundary between regions II and III is formed by the straight line with x intercept $\Gamma(\hat{S})A_{max}/kT$ and slope $(N_{2t} - \Gamma[\hat{S}]A_{max}/kT)$ provided that the slope is positive. If the slope is negative, i.e., if $N_{2t} \leq \Gamma(\hat{S})A_{max}/kT$, then region III simply does not exist and the phase plane has only the first two regions.

In the first region of phase space, Eq. 14 is satisfied, and Eqs. 12a and 12b predict negative values of $\hat{A}$ and $\hat{N}_b$. Simple inspection shows that, since ΔG is an increasing function of N_b and A in region I, the permissible minimum value of ΔG occurs when $\bar{N}_b = \bar{A} = 0$. Inspection also shows that the minimum value of G is independent of S so that $\bar{S}$ in region I is indeterminate in the range $0 \leq S \leq \infty$. It is clear from the nature of this class of solutions that region I is the portion of phase space in which stable cell-cell adhesion cannot occur.

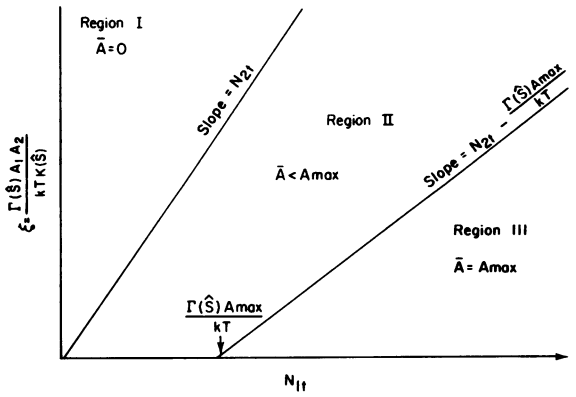

FIGURE 5 Phase diagram for cell-cell adhesion. For model parameters in region I, adhesion is not thermodynamically possible. In region II, adhesion is possible, but the area of contact is $<A_{max}$. In region III, the contact area is at its maximum value, A_{max}.

In Region II of phase space, the inequalities, Eqs. 14 and 15, are both violated. In this case the solutions to Eqs. 11–12b are permissible so that $\bar{N}_b = \hat{N}_b$, $\bar{A} = \hat{A}$ and $\bar{S} = \hat{S}$.

In the third region of phase space, Eq. 14 is violated but Eq. 15 is satisfied. In region III ΔG is minimized by using the constraint condition $\bar{A} = A_{max}$ in place of Eq. 10b and by solving Eq. 10a and 10c simultaneously to determine $\bar{N}_b$ and $\bar{S}$. It is unfortunate that unlike the situation in region II, exact explicit expressions for $\bar{N}_b$ and $\bar{S}$ in region III cannot be obtained. Nevertheless, solutions can easily be computed by standard numerical methods (e.g., simple functional iteration).

In summary, suppose we are given a prescribed set of properties for two potentially adhering cells and we wish to calculate the most probable equilibrium configuration of the system. To do this, we must first determine the phase of the system by calculating $\hat{S}$ and $\xi(\hat{S})$ and by checking inequalities 14 and 15; if Eq. 14 is satisfied and Eq. 15 is violated, then we are in region I and the most probable state is $\bar{A} = \bar{N}_b = 0$ and $\bar{S} = \infty$. If 15 is satisfied and Eq. 14 is violated, then we are in region III and we must numerically solve Eqs. 10a and 10c subject to the constraint $\bar{A} = A_{max}$. Finally, if both Eqs. 14 and 15 are violated, then we are in region II and the most probable equilibrium state is given by $\bar{S} = \hat{S}$, $\bar{A} = \hat{A}$, and $\bar{N}_b = \hat{N}_b$ (i.e., by Eqs. 11–12b).

VARIATIONS AND GENERALIZATIONS

A number of adhesion models that differ slightly from AM-1 can be generated by considering relatively trivial variations in formulation. For example, we could consider nonideal behavior in writing the chemical potentials of the free and bound receptors (Eqs. 4 and 5a); we could also consider higher order terms to the expansion of $\mu_b^0(S)$ (Eq. 5b), and we could consider alternative expressions for parametrizing the repulsive potential between cells. We have examined many possible variations of this kind. In general, the results make for messy mathematics without additional insight. However, in addition to minor variations, there are many thermodynamic models that propose fundamental changes in the structure of AM-1. Some of the more important ways in which other thermodynamic adhesion models differ from AM-1 are the following.

(*a*) Mobility of receptors — AM-1 assumes that the

receptors on both cells are freely mobile. Another important case arises if one of the cells has fixed or immobile receptors. This latter case is probably important in instances of cell-surface adhesion (including adhesion of cells to an extracellular matrix) or in cases of adhesion between viable cells and gluteraldehyde-fixed cells or latex beads. An adhesion model in which receptors on one cell or surface are immobile is given in Dembo and Bell (1984).

(*b*) Multiplicity of receptors — considering the possible multiplicity of receptors can give rise to a number of different special cases. The simplest case arises when there are two classes of receptors on each cell; class W on cell No. 1 forms bridges only with class Y on cell No. 2 and similarly for class X and Z. Obviously the W-Y bridges will in general have different lengths, spring constants, and binding constants than the X-Z bridges. In certain instances competition between the two types of bridges could give rise to a number of different bound states in which some regions of contact are held together predominately by type X-Z bridges and other regions by type W-Y bridges. Thus multiplicity of receptors is probably important in understanding cells (e.g., fibroblasts) that can form two very different types of adherent regions (e.g., close contacts and focal contacts). An example of a model in which each cell has two classes of receptors will be given in a subsequent paper. A different aspect of receptor multiplicity arises in problems of adhesion mediated by lectins, where the saccharide moieties to which the lectins bind may be located at various distances from the cell surface, depending on the structure of the macromolecules of which they are parts.

(*c*) Elastic deformation of cells — AM-1 assumes that the adhering cells are sufficiently fluid, that they are able to deform easily until the area of contact reaches a sharp upper limit, A_{max}. After this limit is reached a further increase in contact is impossible. Obviously, in other circumstances there might be a more gradual increase in resistance to cell deformation as the area of contact increases. In such a case the free energy would include an additional term representing the work done in producing elastic deformation as a function of contact area (e.g., Evans and Skalak, 1980).

(*d*) Mobility of the glycocalyx — AM-1 assumes that the hydrophilic polymer chains that comprise the glycocalyx are somehow anchored at fixed locations in the cell membrane. If some or all of the chains were free to move laterally in the plane of the membrane, then during adhesion, they could theoretically squeeze out of the contact region leading to a reduction in the repulsive potential. The amount of squeezing out would depend on the ease with which material leaving the contact region can be accommodated on the remainder of the cell surface.

The practical importance of this kind of effect is difficult to assess on the basis of currently available data. No redistribution of negative charges was found in the contact area between yeast and *Dictyostelium discoideum* (Ryter and Helio, 1980) as assayed with electron dense markers (cationized ferritin and colloidal iron hydroxide). However, it has been shown (Poo, et al., 1978; Jaffee, 1977) that electric fields will produce an accumulation of lectin receptors towards a pole of the cell. Clearly, lateral redistribution of the glycocalyx could in theory cause very large alterations in the repulsive barrier between cells with profound consequences for cell-cell adhesion.

(*e*) Excluded volume effects for receptors (and glycocalyx) on the same cell-lattice model — AM-1 assumes that there is no interaction between receptors on the same cell and that they form a dilute solution in the membrane, even within the contact area. Hence the chemical potential is taken to have ideal solution form in Eqs. 4 and 5a. However, the number of bonds per unit area, as given by Eq. 10b may then reach very large values. If, for example $\Gamma \approx 10$ ergs/cm^2 (cf., Table I), Eq. 10b predicts $n_b \approx 2.5/(\text{nm})^2$ which may exceed the achievable density of close-packed receptors.

To avoid this difficulty, we have developed a model in which each membrane is subdivided into a number of lattice cells, in each of which there is no more than a single receptor. This model will be published elsewhere. It provides a straightforward way to avoid unrealistically high receptor densities. Moreover, if it is assumed that each lattice cell contains either a receptor or a component of the repulsive glycocalyx, then the lattice model can also allow for excluded volume effects between the glycocalyx and the receptors.

NUMERICAL RESULTS

Table I presents a list of the various parameters that characterize adhering cells according to adhesion model No. 1. This table also presents some preliminary estimates of the parameters. These estimates are subject to considerable uncertainty, but they are useful for purposes of orientation when carrying out illustrative simulations of various experimental systems. The detailed arguments for deriving the estimates given in Table I are presented in the Appendix.

Consider a very general kind of experiment in which the stable configuration of two adhering cells is observed as one or another of the parameters in Table I is varied. AM-1 predicts that such an experiment can produce either a sharp threshold type of transition in the observed configuration if a phase boundary is crossed, or a smooth variation if the phase of the system remains unchanged. The most dramatic phase transition predicted by AM-1 corresponds to the onset of adhesion at the region I–region II boundary (the adhesion boundary). Crossing of the region II–region III boundary corresponds (the maximum contact boundary) to the loss of a degree of freedom due to the onset of maximal contact between the cells. If one cell is much bigger than the other and if the cells have sufficient flexibility, then maximal contact implies the occurrence of phagocytosis.

TABLE I
ESTIMATED PARAMETER VALUES

Parameter	Symbol	Best estimate	Range§
Surface area of cells 1 and 2	A_1, A_2	2×10^{-6} cm^2	10^{-7}–10^{-4}
Maximum contact area	A_{max}	10^{-6} cm^2	0–min(A_1, A_2)
Total receptor numbers on cells 1 and 2	N_{1t}, N_{2t}	10^5/cell	10^3–10^7
Compressibility coefficient of the glycocalyx	γ	10^{-6} dyn	0–10^{-4}
Thickness coefficient of the glycocalyx	τ	10^{-6} cm	0.5–2.0 $\times 10^{-6}$
Binding constant for formation of unstrained cell-cell bridges	K_L	10^{-8} cm^2	10^{-11}–10^{-5}
Unstrained length of cell-cell bridges	L	2×10^{-6} cm	1–3 $\times 10^{-6}$
Force constant for stretching of cell-cell bridges	κ	0.1 dyn/cm	10^{-2}–10^3

*See the Appendix for detailed discussion.
§Same units as for best estimate.

Fig. 6 shows the predictions of AM-1 for how the equilibrium configuration depends on the total number of receptors per cell. In this computation all the parameters except for N_{1t} and N_{2t} were fixed at the values shown in Table I; we then varied the values of N_{1t} and N_{2t} as shown, keeping the ration $N_{1t}/N_{2t} = 1$. To conveniently display the equilibrium configurations of the cells, Fig. 6 makes use of three nondimensional variables. These are (*a*) the fraction of receptors on cell No. 1 or No. 2 that are involved in bridges, $\bar{N}_b/N_{1t} = \bar{N}_b/N_{2t}$, (*b*) the fraction of the maximal contact area that is occupied, $\bar{A}/A_{max}$ and (*c*) the separation distance, normalized by the unstrained bridge length, $(\bar{S} - L)/L$.

The small insert on the right-hand side of Fig. 6 indicates the behavior of the nondimensional variables near to the point where the adhesion boundary is crossed. The behavior of the nondimensional variables when the maximum contact boundary is crossed can be seen in the main part of the figure. Before the adhesion boundary is reached, the separation distance is infinite and both the contact area and the number of bridges are zero. As soon as the adhesion boundary is reached, the separation distance drops to a finite value. Subsequent increases in N_{1t} and N_{2t} do not further decrease the separation distance although there is a rapid increase in both the number of bridges and in the contact area. When N_{1t} reaches the maximum contact boundary at ~6×10^5 mol/cell, further increases in contact area are blocked, but the number of bridges continues to increase; crossing of the maximum contact boundary also causes the separation distance to begin a gradual decline.

In addition to variations in the number of receptors per cell (or per unit surface area of artificial substrate), it is perfectly feasible to conduct experiments in which the number of receptors remains fixed but the repulsive potential or the binding constant is varied. The repulsive potential could be changed by varying the composition of the solvent in such a way as to increase or decrease the steric stabilization effect or by direct modification of the glycocalyx (e.g., by enzymatic treatment). Maneuvers that produce changes in solvent properties or in the number of sugar moieties per unit area of surface should change the compressibility parameter, γ, but should not affect the thickness parameter τ except insofar as the glycocalyx may tend to collapse under reduced hydration or increased salt content. To increase the thickness of the glycocalyx without affecting the compressibility, it would be necessary to

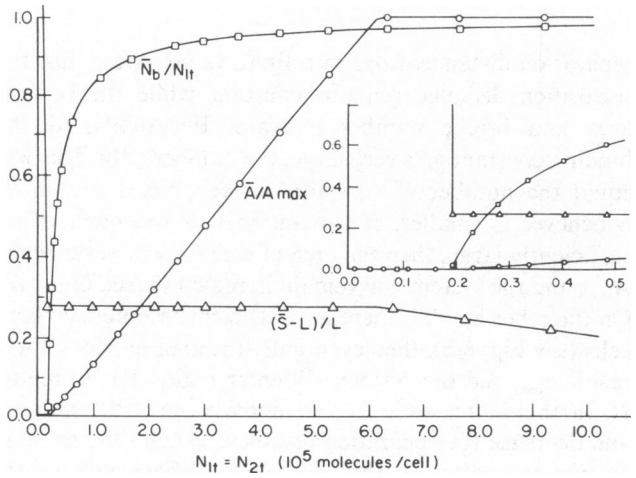

FIGURE 6 Dimensionless contact area (A/A_{max}), number of bonds (N_b/N_{1t}), and separation distance ($\bar{S}/L - 1$) as a function of number of receptors, N_{1t} ($=N_{2t}$). Parameters other than N_{1t} and N_{2t} are as in Table I.

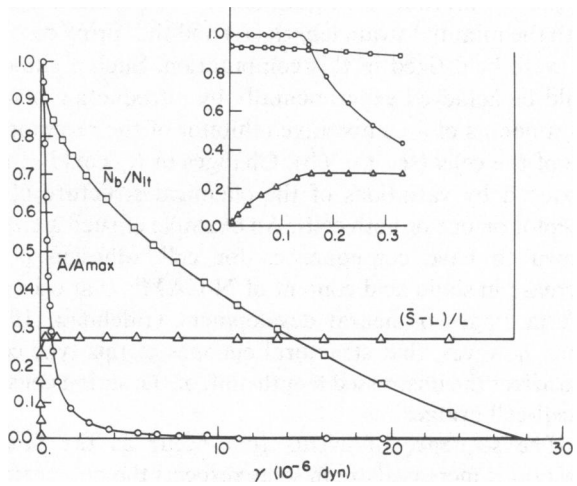

FIGURE 7 Dimensionless contact area, separation distance, and number of bonds as a function of magnitude of the compressibility coefficient, γ. Parameters other than γ are given in Table I.

increase the length of the individual polymer chains, while at the same time decreasing the density of chains so as to leave the total mass of polymer segments per unit area constant.

Fig. 7 shows the prediction of AM-1 for how the equilibrium configuration of cell-cell contact depends on the compressibility parameter (γ) when other parameters are held fixed at the values given in Table I. When γ is very small (see the insert in Fig. 7), it is easy to compress the glycocalyx, the repulsive potential is negligible, and the cells adhere to a maximal extent. In this range of γ values, increasing the parameter causes the cells to be pushed apart slightly, which in turn places stress on the cell-cell bridges. The increased stress on the bridges causes some reduction in the equilibrium number of bridges, but at least initially this reduction is not sufficient to cause a decrease in the contact region (i.e., the system remains in region III of phase space). As γ continues to increase, eventually a critical value of the parameter corresponding to the maximum contact boundary is reached. After this point the area of contact begins to drop and the system enters phase II. As can be seen from the main part of Fig. 7, in region II, increasing the compressibility causes a decline in both the contact area and the number of cell-cell bridges but does not cause any further increase in the separation distance. Comparison of the detailed behavior of $\overline{N}_b/N_{1t}$ and $\overline{A}/A_{max}$ in region II demonstrates that the rate of decline in the contact area as γ increases is much faster than the rate of decline in the number of cell-cell bridges. As γ is made larger and larger, the end result is that the cells are held together by a smaller and smaller toehold containing a very large density of bridges. Eventually, when N_b becomes equal to zero, the separation distance will suddenly jump to infinity, corresponding to the final breaking of cell-cell contact.

Fig. 8 *a* and *b* illustrate the effect of changes in the binding constant for formation of unstressed bridges (K_L) on the equilibrium configuration of two adhering cells. Both the minimal strain length (L) and the spring constant (κ) were held fixed in this computation. Such a situation could be achieved experimentally by introduction of various amounts of a competitive inhibitor of the receptors on one of the cells (see Eq. 6b). Changes in K_L could also be produced by variations of the chemical structure of the receptor on one or both cells. An example of such a change known to have consequences for cell adhesion is the decrease in sialic acid content of N-CAM's that occurs at certain stages of neural development (Edelman, 1983). Note, however, that structural changes of this type could also affect the unstressed length and/or the spring constant of cell-cell bridges.

The sequence of events that occur as the binding constant is increased are in some respects the mirror image of the events that occur as the compressibility increases. When K_L is low, the system is in region I; at a certain critical value the phase I–phase II boundary is crossed and

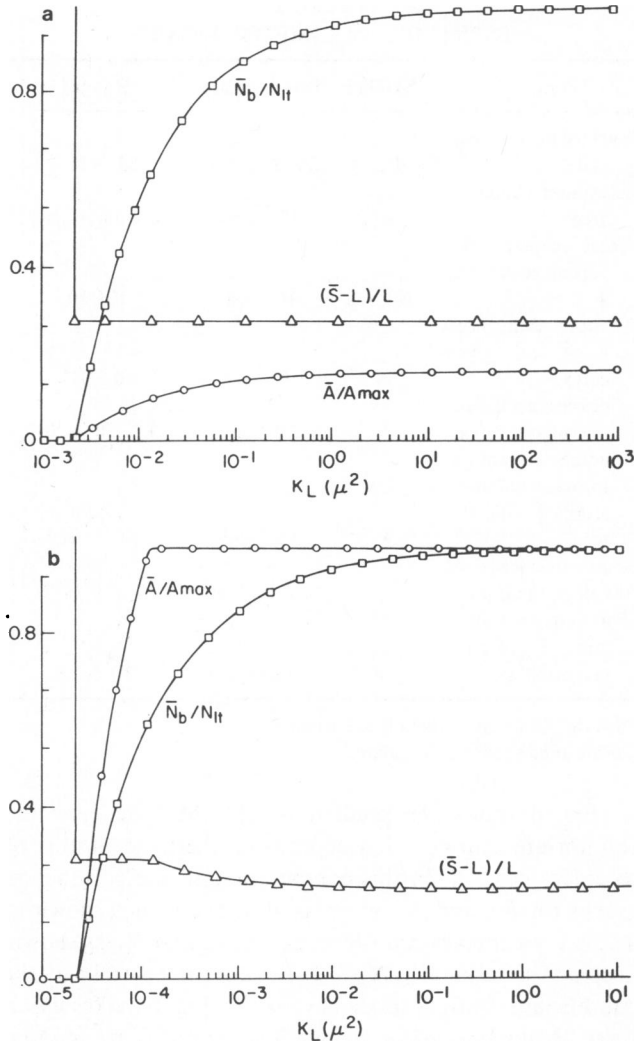

FIGURE 8 (*a*) Dimensionless contact area, separation distance, and number of bonds as a function of the equilibrium constant for bridge formation, K_L. Other parameters are as given in Table I. (*b*) The same as *a* except that $N_{1t} = N_{2t} = 10^6$; in this case it is possible to achieve Phase III binding if K_L is sufficiently large.

separation distance drops to a finite value. After this, the separation distance remains constant while the contact area and bridge number increase. Eventually, as the binding constant gets very large, the number of bridges will equal the number of receptors on cell No. 1 or No. 2, whichever is smaller. If this number of receptors is not sufficiently large, then the area of contact will never reach A_{max}, and the system will remain in region II (see Fig. 8 *a*). On the other hand, if there are sufficient receptors on both cells (see Fig. 8 *b*), then eventually the area of contact will reach A_{max} and the system will enter region III. In region III further increases in K_L will increase the bridge number and decrease the separation distance. When the receptors on one or another of the cells have all been utilized for bridge formation, additional increases in the binding constant will have no further effect.

An aspect of Figs. 6–8 that deserves further comment,

concerns the different manner in which separation distance depends on bridging in phase II vs. phase III. In phase III increasing the number of receptors available for bridging, decreasing the compressibility coefficient, and increasing the binding constant are all associated with a decrease in the cell-cell separation distance. This behavior seems intuitively plausible since maneuvers which favor bridge formation or reduce repulsion, also should cause the two cells to be pulled closer together. The paradox of this interpretation is that in phase II adhesion, the cell-cell separation distance is completely independent of the receptor number, the glycocalyx compressibility, and the binding constant.

A similar example of unexpected behavior in AM-1 concerns the relationship between the thickness parameter τ and the cell-cell separation distance. Naive intuition would suggest that increasing the thickness of the glycocalyx would tend to force the cells apart; however, in region II the exact opposite happens. An increase in τ causes $\bar{S}$ to decrease (see Eq. 11). The reason for this behavior is that increasing τ causes the contact area to shrink very sharply, this compresses a large number of bridges into a small area. This increased density of bonds more than compensates for the increase in repulsion and the cells are pulled closer together.

A further example of unexpected behavior in region II is the lack of any dependence of the number of bridges per unit area, n_b, on the binding constant, $K(S)$. This result follows from Eq. 10b, which may be written $n_b = \Gamma/kT$ and reflects determination of the contact area by a balance between the lateral pressure of the bridges tending to expand it and the compression of the repulsion. Changes of equilibirum constant will change the contact area but not the number of bridges per unit area.

Comparison with Experiment

Obviously, models such as AM-1 and related thermodynamic adhesion models are most directly relevant to studies that report aspects of the physical configuration of individual adherent cells or pairs of cells. In typical studies of this kind, one or more of the observable properties that describe the configuration of adhering cells is measured at various values of the parameters that determine adhesion. For example, Sugimoto (1981) reported increases in the area of adhesion of mouse fibroblasts to artificial substrates as the negative surface charge of the substrates is decreased; Capo et al. (1981) measured the area of contact between macrophages and gluteraldehyde-treated red cells as the surface properties of the red cells were varied by treatment with neuraminidase and polylysine. Michl et al. (1983) measured the depletion of IgG receptors from the upper membrane of macrophages during adhesion to surfaces coated with various densities of IgG.

As a specific example of the analysis of configuration data we will consider some measurements of thymocytes agglutinated by concanavalin A (Con A) (Capo et al., 1982). The protocol in these experiments called for incubating the cells with various amounts of Con A so as to achieve different levels of tightly bound Con A molecules per cell. The exact amount of Con A binding achieved by a given incubation was quantitatively determined in separate binding studies. These binding studies also indicated that the total number of Con A binding sugar moieties per thymocyte was $\approx 10^6$. After exposure to Con A the cells were washed, centrifuged into a pellet, resuspended, and fixed for electron microscopy. Thus, in the final moment before fixation, a pair of adhering cells both had an equal number of tightly bound Con A molecules capable of forming bridges by binding with sugar moieties on the other cell. By measurements on a large number of sectioned cells, the dependence of the area of contact on the number of Con A molecules per cell was determined.

Application of AM-1 to the data of Capo et al. (1982) is considerably simplified because the number of one species of receptor (i.e., sugar moieties) is always considerably larger than the number of the other species (i.e., Con A molecules). If we let N_{1t} equal the number of Con A

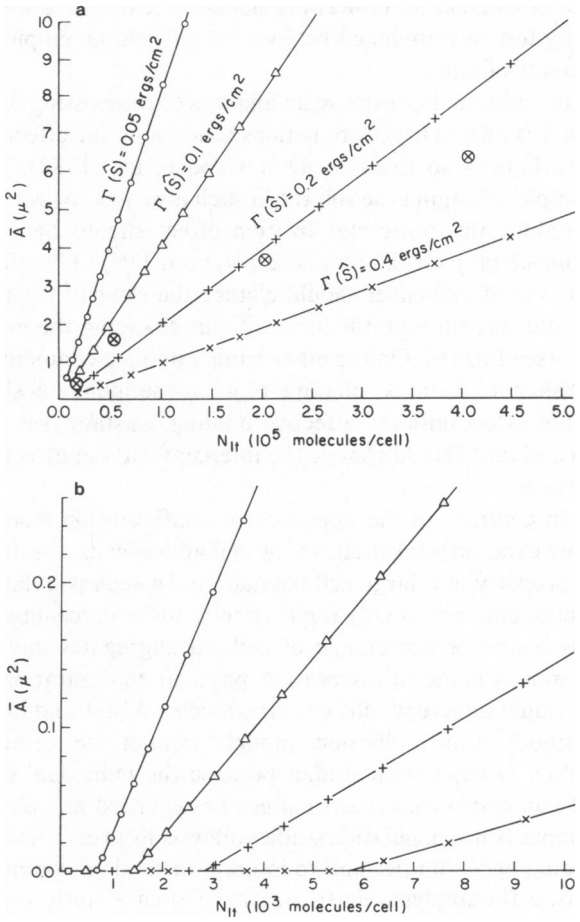

FIGURE 9 (*a*) Contact area in μ^2 as a function of number of Con A mol/cell. Data points, ×, are from the experiments of Capo et al., 1982. Theoretical curves show predictions of Eq. 12b for several values of $\Gamma(\hat{S})$. Other parameters in Eq. 12b are taken from Table I. (*b*) Behavior of the theoretical curves from Fig. 9 *a* at very low levels of cell-cell contact.

molecules per cell and N_{2t} equal the number of complementary sugar moieties per cell, then it is easy to see that if $N_{2t} > N_{1t}$, Eq. 12b reduces to the simple linear expression

$$\bar{A} \simeq \frac{kTN_{1t}}{\Gamma(\hat{S})} - \frac{A_1A_2}{K(\hat{S})N_{2t}}. \quad (16)$$

As Eq. 16 explicitly shows, the slope of a plot of $\bar{A}$ as a function of N_{1t} yields information on the phase II repulsive potential $\Gamma(\hat{S})$; whereas the intercept yields information on the phase II binding constant $K(\hat{S})$.

Fig. 9 *a* shows the data of Capo et al. (1982) as well as the predictions of Eq. 16 for the dependence of $\bar{A}$ on N_{1t} for several values of the phase II repulsive potential $\Gamma(\hat{S})$. In each of these curves, N_{2t} was fixed at 10^6, and all other parameters are as given in Table I. As can be seen, a value of $\Gamma(\hat{S}) \approx 0.20$ ergs/cm^2 gives a good fit to the data. Note that this value of the phase II repulsive potential is in reasonable agreement with the independent theoretical estimates derived by Bongrand and Bell (1984) for the repulsive potential at separation distances of 200 Å.

Fig. 9 *b* shows an enlarged view of the theoretical curves in Fig. 9 *a* at small values of N_{1t}. It is regrettable that the data of Capo et al. (1982) are not sufficiently accurate to really test this predicted behavior or to yield an empirical estimate of $K(\hat{S})$.

In addition to providing an analysis of the existing data, AM-1 is able to make predictions concerning the effects of perturbations to the system of Capo et al. (1982). For example, changing the solvent in such a way as to increase or reduce the steric stabilization effect should have an influence only on the repulsive potential $\Gamma(\hat{S})$. Therefore, this kind of maneuver should change the slope of the best straight line through the data without changing the intercept (see Eq. 16). On the other hand, adding a competitive inhibitor of Con A binding (e.g., α-methylmannoside) should affect only the effective binding constant (see Eq. 6b) and thus should change the intercept without affecting the slope.

In contrast to the approach of configuration studies, many experimental studies view cell adhesion as a statistical property of a large cell population. In such population studies, data are usually reported in terms of percentage of cells bound or percentage of cells in aggregates and no attempt is made to discern the physical configuration of individual adherent cells or pairs of cells. AM-1 and other thermodynamic adhesion models cannot be directly applied to population studies because the individual cell-cell and cell-surface pairs cannot be regarded as isolated systems. Since population studies allow cells to compete for binding opportunities and to interact in random combinations, a thermodynamic treatment of such a study would require minimization of the free energy of the population as a whole. Even if this were done, however, it is doubtful that the global equilibrium of a population could be reached on a time scale short compared with the time scale for metabolic processes.

In addition to these fundamental difficulties, population studies usually regard a cell as bound if it remains attached to another cell or to a surface after some kind of standardized agitation and washing procedure. Such an essentially arbitrary experimental definition is more demanding than the mere existence or nonexistence of a stable bound state. In addition to existence, the bound state must have enough stability to resist mechanical disruption.

Despite the problems, there are circumstances in which the average behavior of a random mixture of cells will give direct information on the most probable behavior of an individual pair of cells. For example, suppose that the cells of a population are fairly homogeneous with regard to the properties that affect adhesion and that the agitation procedure used to remove nonadherent cells does not disrupt cells held by more than a few bonds (see Bell, 1978, for a discussion of the forces required to break typical adhesive bonds). Clearly if a stable bound state of individual pairs of cells does not exist, then both configuration studies and population studies will detect zero binding. On the other hand, if a stable state does exist, a population approach should detect at least some fraction of bound cells. Thus, population studies are well-suited for detecting and measuring the adhesion threshold predicted by AM-1 as well as by other thermodynamic adhesion models. In a similar way, the population approach can be useful for detecting the maximum contact boundary in studies of phagocytosis; a good example of this kind is the paper by Beukers et al. (1978) on the inhibition of phagocytosis of polystyrene spherules with increasing amounts of absorbed albumin.

An illustration of a quantitative population type system in which the threshold for onset of cell adhesion is readily studied was reported by Weigel et al. (1979). These workers showed that rat hepatocytes possess specific receptors for galactosyl moieties; whereas chicken hepatocytes have receptors that bind only *N*-acetylglucosaminyl moieties. It was also shown that rat and chicken hepatocytes would adhere to flat polyacrylamide gels provided the appropriate sugar moieties were covalently incorporated into the gel. Various methods of linking the sugar to the gel were tried; however, the length of the spacer and the method of synthesis had no material impact on the results obtained. The procedure used to remove unbound cells from the gel also had a very small effect on the results.

By varying the concentration of sugar incorporated into the gels, Weigel et al. (1979) observed a threshold concentration at which cell adhesion first occurred. The amount of adhesion sharply increased after the first onset, and adhesion appeared to be maximal at concentrations 10 to 20% higher than the threshold level; adhesion was undetectable at levels even marginally below the threshold. In further studies, Weigel et al. (1979) found that the addition of small amounts of a competitively binding free sugar to the solution bathing the cells caused a shift in the threshold for onset of cell binding towards higher densities

of incorporated sugar. The amount of shift in the threshold was a linear function of the concentration of competing sugar added; noncompeting sugars had no effect on adhesion.

We interpret the results of Weigel et al. (1979) as strong confirmation of the existence of the kind of threshold transition for onset of cell adhesion shown in Fig. 6. Note, however, that the adhesion point may not be easy to observe in all cases. Depending on the particular parameters of the systems, the critical receptor numbers required for the onset of adhesion could be quite small and the increase in binding after the onset of adhesion could be more gradual than seen by Weigel et al. (1979).

AM-1 is not an appropriate model for describing the system of Weigel et al. (1979), since one class of receptor (i.e., the sugar moieties) are immobile. The correct model (AM-2) is given by Dembo and Bell (1984) where it is shown that a threshold for adhesion still occurs when one species of receptor is immobile, although the conditions that govern this threshold are different than in the case of AM-1. According to AM-2 the adhesion boundary in the experiments of Weigel et al. (1979) is given by

$$\langle n_{1t} \rangle_t = \frac{\Gamma(\hat{S})/kT}{\ln [1 + K(\hat{S})N_{2t}/A_2]}, \tag{17a}$$

where $\langle n_{1t} \rangle_t = N_{1t}/A_1$ is the critical density of sites on the gel, N_{2t} is the total number of complementary receptors per cell and A_2 is the surface area of a cell. If $K(\hat{S})N_{2t}/A_2$ is not too large compared with one, then Eq. 17a can be replaced by the simpler expression

$$\langle n_{1t} \rangle_t \simeq \frac{\Gamma(\hat{S})A_2}{kTK(\hat{S})N_{2t}}. \tag{17b}$$

To see the effect of competitive inhibitors on the threshold level, we must replace the value of $K(\hat{S})$ in Eq. 17b by the effective binding constant (Eq. 6b). From the resulting expression, it is easy to see that, as reported by Weigel et al. (1979), the threshold is a linear function of the inhibitor concentration. However, in addition to this after the fact agreement, Eq. 17b allows the K_i of the inhibitor to be calculated from the data of Weigel et al. (1979). This value of K_i should agree with values of K_i obtained by direct studies of inhibitor binding. Eq. 17b also predicts that the threshold density of sugar in the gel should depend inversely on the number of complementary receptors on the cells and should increase linearly as the repulsive forces between the cells and the gel are increased.

In principle, another approach for testing thermodynamic adhesion models could be taken using techniques that have been developed for directly measuring the force between two surfaces bearing adsorbed macromolecules in liquid media (see Klein, 1983, for a recent report and references to earlier work). To simulate cell-cell interactions, the adsorbed polymer layers would need to resemble cell surfaces. Also, for comparison with the present models, the receptors on at least one of the surfaces would need to be mobile. In addition, Evans and Leung (1984) have manipulated cells attached to micropipettes to measure contact areas and forces for detachment.

DISCUSSION

In this paper we have developed a family of thermodynamic models for describing adhesion between two cells or between a cell and a surface. These models provide the user with a powerful method for integrating various notions about the complementary receptors on the two surfaces (e.g., lateral mobility, heterogeneity, total number per cell), notions about the cell-cell bridges that mediate adhesion (e.g., spring constant, length, binding constant), notions about the repulsive forces between cells (e.g., compressibility of the glycocalyx, thickness of the glycocalyx, lateral mobility of the glycocalyx), and notions about the purely geometrical parameters of adhesion (e.g., maximum contact area, total surface areas of the two cells, heterogeneity vs. uniformity of contact distance).

To achieve the simplicity and generality of a thermodynamic approach, a price must be paid in terms of certain definite limitations. One such limitation is embodied in the negligible metabolism hypothesis. In essence, this hypothesis means that our models do not take into account the possibility that cells might somehow actively grip each other with continual expenditure of energy (Rees et al., 1977). Nor can our approach account for the possibility that cells will in some manner actively try to pull away from each other. Finally, a thermodynamic description of adhesion requires that the basic parameters of the cells that affect adhesion (see Table I) do not change rapidly with time.

In addition to the above limitations, it is important to emphasize that thermodynamic models say nothing about the kinetic process involved in reaching equilibrium. In some cases a chance thermal fluctuation in the number of receptors may be required to nucleate a small site of adhesion, which then grows, due to thermal motions of the membranes in a zipper-like fashion. In other cases, active motions of one or another of the cells could be involved in both the initiation and propagation of adhesion. Paradoxically, the ability of cells to undergo active motions and deformations that increase or decrease the contact area can be very important in influencing the kinetic process of adhesion without constituting a violation of the negligible metabolism hypothesis as far as the equilibrium state of adhesion is concerned. In light of the obvious analogy with a well-known Southern folktale, this paradox may be called the "tar baby" effect (Harris, 1955).

The tar baby effect constitutes an important consideration when interpreting experiments relating to the influence of metabolic inhibitors on adhesion. If adhesion is decreased by metabolic inhibitors, then one must be sure to eliminate kinetic effects before concluding that cells are capable of active grip or some similar phenomenon. A

simple way to check for a kinetic involvement of metabolism is to add inhibitors both before and after adhesion has been allowed to proceed. If the end result is independent of the time sequence of the experiment, then the tar baby effect can be eliminated.

Obviously, with all the possibilities inherent in thermodynamic adhesion models, it is unrealistic to analyze more than a few special cases in detail or to talk with too much confidence about general properties of adhesion. Nevertheless, there are several conclusions that are robust in the sense that they seem to be true in all but a relatively few special cases.

One such conclusion is that bridging receptors will become concentrated in regions of cell-cell or cell-substrate contact. Such accumulations of receptors in contact areas have been observed (e.g., Singer, 1976), deduced from the forces required to disrupt aggregates (Capo et al., 1982), and are expected quite generally (Bell, 1979). In view of the well-known functions of receptor aggregation in immunological systems, such accumulation of receptors could serve as a transduction mechanism for triggering various cell responses (e.g., phagocytosis, exocytotic granule release). Redistribution of receptors could also serve as a signal for polarization of the cell membrane relative to the site of adhesion. Insofar as internal cell structures, e.g., cytoskeletal elements, can sense this polarization (Edelman, 1976; Bourguignon and Singer, 1977), the interior of the cell can also be polarized. In this connection it is logical to suppose that specialized cell-cell junctions, such as synapses, tight junctions, and gap junction could be the natural consequences of receptor accumulation in regions of cell-cell contact, with details of the junction to be affected by specifics of the receptors and their interactions with each other and other molecules on a cell.

Another robust conclusion of our analysis is the pervasive presence of various phase transitions in cell adhesion. The existence of these transitions makes it clear that cells cannot be regarded as sticky billiard balls that aggregate according to simple laws of mass action. Unlike the case of billiard balls, contact between cells can be stabilized by highly cooperative rearrangements of the internal variables of the cells. In many ways the adhesion of cells is analogous to the interaction of two immiscible liquid droplets (Torza and Mason, 1968; Van Oss et al., 1975). However, in the case of liquid drops, interactions are described in terms of interfacial surface tensions between the two drops and between each drop and the surrounding fluid, and conditions are found in which two drops will adhere or in which one drop will engulf the other. Because no constraint is placed on the surface area of either drop, it is possible for the smaller drop to engulf the larger. For interacting drops, there is, of course, no surface material to form specific bonds and accumulate in the contact area. Engulfment of one liposome by another bearing complimentary receptors has also been observed (Haywood, 1974).

In various studies of cell adhesion, one observes a change in adhesiveness as a corollary of a more general biological phenomenon (e.g., neoplastic transformation). In such a case the problem is to deduce what of many factors could be causing the change in adhesiveness. Thermodynamic adhesion models can be useful in this regard since as we have seen, naive intuition is an unreliable guide to the significance of various parameter changes. In addition, it is frequently possible to eliminate certain causative factors with data of a simple quantitative nature.

APPENDIX

Estimation of Parameter Values

Cell Surface Areas A_1 and A_2. The areas of some representative cells are: 70 μ^2 for a red blood cell, ~200 μ^2 for a small lymphocyte and ~2,500 μ^2 for a macrophage (Michl et al., 1983).

Maximum Contact Area; A_{max}. A_{max} must, of course, be smaller than or equal to the area of the smaller cell. However, as illustrated in Fig. 10, A_{max} is also dependent on the degree of fluidity of the cytoskeletal architecture of the two cells as well as on the surface-to-volume ratio of the cells.

Receptor Numbers N_{1T} and N_{2T}. Receptor numbers can, of course, vary greatly depending on the particular cells under consideration. 10^6 or 10^7 mol/cell is an upper limit for small cells such as a lymphocyte. Such numbers would be reached by abundant surface species such as Con A receptors. For sparsely distributed receptors, such as surface immunoglobin molecules, there could be as few as 10^3 or 10^4 per cell.

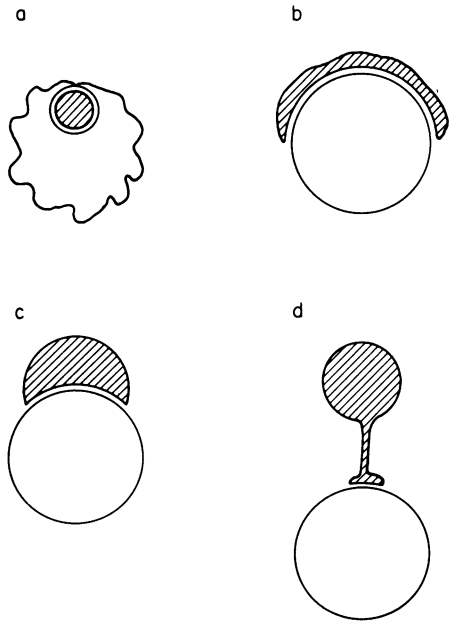

FIGURE 10 The maximum contact area between two cells may depend on cytoskeletal rigidity and other constraints on membrane bending in one or both cells.

Compressibility of the Glycocalyx, γ. According to the Flory-Krigbaum theory of steric stabilization (Bongrand and Bell, 1983; Napper, 1977), the compressibility coefficient of the glycocalyx can be approximated by an expression of the form

$$\gamma \simeq 2\kappa T(V_s^2/V_1)(N_{S1} + N_{S2})^2(1/2 - \chi). \quad (A1)$$

In this equation, V_s equals the volume of a polymer segment, V_1 equals the volume of a water molecule, N_{S1} and N_{s2} equals the number of polymer segments per unit area of the glycocalyx on cells 1 and 2, respectively, and χ equals an interaction parameter measuring the degree of solubility of the polymer in the solvent.

If we estimate that water is a good solvent for polysaccarides ($\chi \cong 0$), that the volume of a typical saccaride moiety of the glycocalyx is $V_s \cong 3 \times 10^{-22}$ cm^3, and that there are ~0.5 saccaride residues/nm^2 of cell surface, then we calculate from Eq. A1 that γ is $\sim 10^{-6}$ dyn.

Thickness of the Glycocalyx, τ. τ measures the cell-cell separation distance at which the repulsive polymer layers coating cells No. 1 and cells No. 2 are interpenetrated by ~50%. Because the thickness of the glycocalyx on a typical cell is ~10 nm, we can safely estimate that τ is somewhere between 5 and 20 nm.

Equilibrium Constant for Unstrained Bridge Formation, K_L. Suppose that the equilibrium constant for binding between the two species of receptors is given by K_S, if one or both of the receptors is free in solution. If K_S is known, then according to Bell (1978) we can estimate the binding constant when both receptors are anchored at one end to a lipid membrane as

$$K_L \cong K_S/\sigma, \quad (A2)$$

where σ is the thickness of the confinement region to which the two species of receptor sites are restricted. Taking $K_S \cong 10^6$ M$^{-1} \cong 10^{-15}$ cm^3, and $\sigma \cong 10^{-7}$ cm, we calculate from Eq. A2 that $K_L \sim 10^{-8}$ cm^2 = 1 μ^2. Clearly, however, this estimate of K_L could easily increase or decrease by a factor of 100 or 1,000 since the values of K_S and σ are quite variable.

Unstrained Length of a Cell-Cell Bridge, L. The gap between the membrane surfaces of adhering cells is typically in the range of 10–20 nm. Obviously, this range also represents the approximate range of L values.

Spring Constant of a Cell-Cell Bridge, κ. Several authors (Levy and Karplus, 1979; Suezaki and Gō, 1976) have presented detailed calculation of the Youngs' modules for stretching of α-helical protein segments. For an α-helix of length L, the spring constant is related to the Youngs' modules by the expression

$$\kappa \equiv \epsilon a/L, \quad (A3)$$

where ϵ equals Youngs' modules ($\sim 2 \times 10^{11}$ dyn/cm) and a equals the cross-sectional area (5.15×10^{-15} cm^2). Based on Eq. A3, we calculate that if a cell-cell bridge contains a series of α-helical segments of ~10 nm in total length, then $\kappa \cong 10^3$ dyn/cm.

α helices are probably among the most rigid and highly stabilized protein structures.) The inevitable presence of other random coil regions of protein structure could greatly reduce the value of κ. As a lower limit on κ, we can consider the spring constant for deformation of a freely jointed random coil

$$\kappa \approx kT/L^2. \quad (A4)$$

The use of Eq. A4 yields a value of $\sim 10^{-2}$ dyn/cm. We thus conclude that 0.1 dyn/cm is a reasonable first estimate of κ, but that this parameter could vary between 10^{-2} and 10^3 dyn/cm.

We are indebted to the Aspen Center for Physics for hospitality, where this work was started, and to P. Salamon and S. Silverstein for comments on the manuscript.

M. Dembo was partially supported by a Research Career Development Award, 1-K04-AI0056-01. This work was supported by the U. S. Department of Energy.

Received for publication 7 October 1983 and in final form 9 January 1984.

REFERENCES

Bell, G. I. 1978. Models for the specific adhesion of cells to cells. *Science (Wash. DC)*. 200:618–627.

Bell, G. I. 1979. Theoretical models for cell-cell interactions in immune responses. *In* Physical Chemical Aspects of Cell Surface Events in Cellular Regulation. C. DeLisi and R. Blumenthal, editors. Elsevier/North-Holland, New York. 371–393.

Beukers, H., F. A. Deierkauf, C. P. Blom, M. Deierkauf, and J. C. Riemersma. 1978. Effects of albumin on the phagocytosis of polystyrene spherules by rabbit polymorphonuclear leucocytes. *J. Cell Physiol.* 97:29–36.

Bongrand, P., and G. I. Bell. 1984. Cell-cell adhesion: parameters and possible mechanisms. *In* Cell Surface Dynamics: Concepts and Models. C. DeLisi, A. Perelson, and F. Wiegel, editors. Marcel Dekker, Inc., New York. In press.

Bongrand, P., C. Capo, and R. Depieds. 1982. Physics of cell adhesion. *Prog. Surf. Membr. Sci.* 12:217–285.

Bourguignon, L. Y. W., and S. J. Singer. 1977. Transmembrane interaction and the mechanism of capping of surface receptors by their specific ligands. *Proc. Natl. Acad. Sci. USA.* 74:5031–5035.

Capo, C., P. Bongrand, A. M. Benoliel, A. Ryter, and R. Depieds. 1981. Particle-macrophage interaction: role of surface charge. *Ann. Immunol.* 130D:165–173.

Capo, C., F. Garrouste, A. M. Benoliel, P. Bongrand, A. Ryter, and G. Bell. 1982. Concanavalin-A-mediated thymocyte agglutination: a model for a quantitative study of cell adhesion. *J. Cell Sci.* 56:21–48.

Dembo, M., and G. Bell. 1984. Thermodynamics of cell adhesion. *Cur. Top. Membr. Transp.* 22:000–000.

Edelman, G. M. 1976. Surface modulation in cell growth. *Science (Wash. DC)*. 192:218–226.

Edelman, G. M. 1983. Cell adhesion molecules. *Science (Wash. DC)*. 219:450–457.

Evans, E., and A. Leung. 1984. Adhesivity and rigidity of erythrocyte membrane in relation to wheat germ agglutinin binding. *J. Cell Biol.* 98:1201–1208.

Evans, E. A., and R. Skalak. 1980. Mechanics and Thermodynamics of Biomembranes. CRC Press, Boca Raton, FL.

Frazier, W. A., L. Glaser, and D. I. Gottlieb. 1982. Cellular Recognition. Alan R. Liss, Inc., New York.

Gingell, D., and S. Vince. 1980. Cell Adhesion and Motility. A. S. G. Curtis and L. D. Pitts, editors. Cambridge University Press. 39–64.

Grinnell, F. 1974. Studies on the mechanism of cell attachment to a substratum with serum in the medium: further evidence supporting a requirement for two biochemically distinct processes. *Arch. Biochem. Biophys.* 165:524–530.

Harris, J. C. 1955. Complete Tales of Uncle Remus. Richard Chase, editor. Houghton Mifflin Co., New York.

Haywood, A. M. 1974. Fusion of sendai viruses with model membranes. *J. Mol. Biol.* 87:625–628.

Hill, T. L. 1960. An Introduction to Statistical Thermodynamics. Addison-Wesley Publishing Co., Inc., Reading, MA.

Jaffee, L. F. 1977. Electrophoresis along cell membranes. *Nature (Lond.)*. 265:600–602.

Klein, J. 1983. Forces between mica surfaces bearing adsorbed macromolecules in liquid media. *J. Chem. Soc. Faraday Trans.* 79:99–118.

Levy, R. M., and M. Karplus. 1979. Vibrational approach to the dynamics of an α helix. *Biopolymers.* 18:2465–2495.

Michl, J., M. M. Pieczonha, J. C. Unkeless, G. I. Bell, and S. C. Silverstein. 1983. Fc receptor modulation in mononuclear phagocytes maintained on immobilized immune complexes occurs by diffusion of the receptor molecules. *J. Exp. Med.* 157:2121–2130.

Napper, D. H. 1977. Steric stabilization. *J. Colloid Interface Sci.* 58:390–407.

Nir, S., and M. Andersen. 1977. Van der Waals interactions between cell surfaces. *J. Membr. Biol.* 31:1–18.

Parsegian, V. A. 1973. Long-range physical forces in the biological milieu. *Annu. Rev. Biophys. Bioeng.* 2:221–255.

Poo, M-M., W-J. Poo, and J. W. Lam. 1978. Lateral electrophoresis and diffusion on concanavalin A receptors in the membrane of embryonic muscle cell. *J. Cell Biol.* 76:483–501.

Rees, D. A., C. W. Lloyd, and D. Thom. 1977. Control of grip and stick in cell adhesion through lateral relationships of membrane glycoproteins. *Nature* (*Lond.*). 267:124–128.

Ryter, A., and R. Hellio. 1980. Electron microscopic study of *dictyostelium discoideum* plasma membrane and its modifications during and after phagocytosis. *J. Cell Sci.* 41:75–87.

Singer, J. S. 1976. The fluid mosaic model of membrane structure: some applications to ligand-receptor and cell-cell interactions. *In* Surface Membrane Receptors. R. A. Bradshaw, W. A. Frazier, R. C. Merrell, D. I. Gottlieb, and R. A. Hogue-Angletti, editors. Plenum Publishing Corp., New York. 1–24.

Springer, W. R., and W. R. Barondes. 1982. Evidence for another cell-adhesion molecule in *Dictyostelium discoideum. Proc. Natl. Acad. Sci. USA.* 79:6561–6565.

Suezaki, Y., and M. Gō. 1976. Fluctuations and mechanical strength of α helices of polyglycine and poly (L-alanine). *Biopolymers.* 15:2137–2153.

Sugimoto, Y. 1981. Effect on the adhesion and locomotion of mouse fibroblasts by their interacting with differently charged substrates. A quantitative study by ultrastructural methods. *Exp. Cell Res.* 135:39–45.

Torza, S., and S. G. Mason. 1968. Coalescence of two immiscible liquid drops. *Science* (*Wash. DC.*). 163:813–814.

Van Oss, C. J., C. F. Gillman, and A. W. Neumann. 1975. Phagocytic Engulfment and Cell Adhesiveness as Cellular Surface Phenomena. Marcel Dekker Inc., New York.

Weigel, P. H., R. L. Schnaar, M. S. Kahlenschmidt, E. Schmell, R. T. Lee, Y. C. Lee, and S. Roseman. 1979. Adhesion of hepatocytes to immobilized sugars — a threshold phenomenon. *J. Biol. Chem.* 254:10830–10838.